H3K9 methylation maintains female identity in *Drosophila* germ cells through repression of the spermatogenesis program

Anne E. Smolko, Laura Shapiro-Kulnane, Helen K. Salz*

Department of Genetics and Genome Sciences, Case Western Reserve University School of Medicine, Cleveland, OH 44106-4955, USA.

Correspondence to and Lead Contact: Helen K. Salz, PhD, (216) 368-2879; hks@case.edu

Key words: facultative heterochromatin, sex determination, cell fate memory, sex-specific transcriptional regulation, oogenesis, germline tumors, SETDB1, HP1, PHF7, SXL

Summary

Maintaining germ cell sexual identity is critical for gametogenesis. We find that Drosophila female germ cells employ H3K9me3 marked euchromatin, operationally defined as facultative heterochromatin, in the silencing of sex-inappropriate protein-encoding genes. In female germ cells the H3K9 trimethylase SETDB1, its binding protein WDE, and the H3K9 binding protein HP1a, are required for spermatogenesis gene silencing. SETDB1 controls the accumulation of H3K9me3 marks over a subset of these silenced genes, without spreading into neighboring loci. Regional deposition is especially striking at *phf7,* a male germline gene whose repression is known to be necessary for maintaining female identity. Furthermore, H3K9me3 recruitment to *phf7* and other spermatogenesis genes is dependent on the female sex determination gene *Sxl.* Together our work reveals an H3K9me3 epigenetic mechanism necessary to ensure the stability of female germ cell identity, highlighting the emerging importance of H3K9me3 marked euchromatin in maintaining cell fate.

Introduction

In metazoans, germ cell development begins early in embryogenesis when the primordial germ cells are specified as distinct from somatic cells. Specified primordial germ cells then migrate into the embryonic gonad, where they begin to exhibit sex-specific division rates and gene expression programs, ultimately leading to meiosis and differentiation into either eggs or sperm. Defects in sex-specific programming interferes with germ cell differentiation leading to infertility and germ cell tumors. Successful reproduction, therefore, depends on the capacity of germ cells to maintain their sexual identity in the form of sex-specific regulation of gene expression (Lesch and Page, 2012; Salz et al., 2017; Spiller et al., 2017).

In *Drosophila melanogaster,* germ cell sexual identity is determined in embryogenesis by the sex of the developing somatic gonad (Casper and Van Doren, 2009; Horabin et al., 1995; Staab et al., 1996; Wawersik et al., 2005). However, extrinsic control is lost after embryogenesis and sexual identity is maintained by a cell-intrinsic mechanism (Casper and Van Doren, 2009). The SEX-LETHAL (SXL) female-specific RNA binding protein is an integral component of this cell-intrinsic mechanism as its absence leads to a global upregulation of spermatogenesis genes and a germ cell tumor phenotype (Chau et al., 2009; Schüpbach, 1985; Shapiro-Kulnane et al., 2015). Previous studies have shown that the tumor phenotype is directly linked to the acquisition of male-like characteristics; *e.g.* ectopic expression of the testis-specific *PHD finger protein 7 (phf7)* (Shapiro-Kulnane et al., 2015). Germ cells lacking SXL protein ectopically express PHF7 protein, and PHF7 depletion in these mutants suppresses the tumor phenotype, restoring oogenesis. Sex-specific regulation of *phf7* is particularly important because ectopic expression of PHF7 protein in a wild-type background is sufficient to disrupt female germ cell fate. This finding is consistent with previous studies that identified *phf7* as a male germline sexual identity gene (Yang et al., 2012). While these genetic studies reveal that *Sxl* is required for silencing *phf7* and other spermatogenesis genes, regulation proved to be indirect. Consequently, the mechanism(s) controlling sex-specific gene expression in germ cells remains unknown.

Here, we show that female germ cell fate is maintained via an epigenetic regulatory pathway in

which SETDB1 (aka EGGLESS) is the required chromatin writer and that *phf7* is one of the key spermatogenesis genes silenced by SETDB1. SETDB1 trimethylates H3K9 (H3K9me3), a feature of heterochromatin (Brower-Toland et al., 2009; Elgin and Reuter, 2013). Using tissue-specific knockdown approaches we establish that SETDB1, its protein partner WINDEI [WDE, aka ATF7IP (Koch et al., 2009; Timms et al., 2016)] and the H3K9me3 reader, Heterochromatin binding protein 1a [HP1a, encoded by the *Su(var)205* locus (Eissenberg and Elgin, 2014)], are required for silencing *phf7* and other spermatogenesis genes. We further find that H3K9me3 repressive marks accumulate on a select subset of these genes in a SETDB1 dependent manner. SETDB1 dependent H3K9me3 deposition is highly localized and does not spread into neighboring loci. Regional deposition is especially striking at the *phf7* locus with its two sex-specific transcription start sites (TSS), where H3K9me3 accumulation is restricted to the region surrounding the silent testis specific TSS. Lastly, H3K9me3 recruitment to *phf7* and other spermatogenesis genes is dependent on *Sxl.* By establishing how female germ cell identity is maintained our studies highlight the emerging role of H3K9me3 marked chromatin in silencing protein-encoding genes.

Results

H3K9me3 pathway members are required for germ cell differentiation

H3K9me3 marked chromatin has recently emerged as a player in maintaining cell identity by silencing lineage-inappropriate protein-encoding genes (Becker et al., 2016). We therefore investigated the potential involvement of H3K9me3 in spermatogenesis gene silencing. We first tested whether H3K9me3 localization was disrupted in germ cells lacking SXL protein. As with our earlier studies, we take advantage of the viable *sans-fille*^{148} (*snf*^{148}) allele to selectively eliminate SXL protein in germ cells without disrupting function in the surrounding somatic cells (Chau et al., 2009; 2012; Nagengast et al., 2003; Shapiro-Kulnane et al., 2015). The intense H3K9me3 staining observed in wild-type germ cells is abolished in *snf*^{148} mutant germaria (Figures 1A and 1B). This observation suggests a link between maintenance of sex identity and H3K9me3.

Previous studies reported that loss of the H3K9 trimethylase SETDB1 leads to mutant germaria filled with undifferentiated germ cells, characteristic of a germ cell tumor phenotype (Clough et al., 2007; Rangan et al., 2011; Wang et al., 2011; Yoon et al., 2008). To confirm and extend these studies, we analyzed the consequences of depleting SETDB1, the SETDB1-interacting protein WDE (Koch et al., 2009; Timms et al., 2016), and the H3K9me3 binding protein HP1a (Eissenberg and Elgin, 2014), in germ cells by cell type RNA interference (RNAi). We achieved GermLine specific KnockDown (*GLKD*) with *nos-Gal4*, a strong driver largely restricted to pre-meiotic germ cells (Van Doren et al., 1998). As expected, *setdb1 GLKD* and *wde GLKD* abolished the intense H3K9me3 staining foci observed in wild-type germ cells (Figures 1C and 1D).

The oogenesis defects elicited by *setdb1, wde,* and *hp1a GLKD* are similar, as judged by the number of round spectrosome like structures present in the germarium (Figure S1). The spectrosome is a spherical α-Spectrin-containing structure that is normally found only in germline stem cells (GSCs) and its differentiating daughter cell, the cystoblast (~5 per germarium). As differentiation proceeds, the round spectrosome elongates and branches out to form a fusome. We find that the majority of *setdb1, wde,* and *hp1a GLKD* mutant germaria contain 6 or more spectrosome containing germ cells. This indicates that loss of H3K9me3 pathway members leads to a germ cell tumor phenotype.

Loss of H3K9me3 pathway members in female germ cells leads to ectopic spermatogenesis gene expression

To gain an understanding of the defects associated with the loss of H3K9me3 pathway components in germ cells, we used high throughput sequencing (RNA-seq) to compare the transcriptomes of *GLKD* mutant ovaries with wild-type ovaries from newborn (0-24 hour) females. Newborn ovaries lack late stage egg chambers, establishing a natural method for eliminating many of the cell types not present in tumors.

Genes that change expression at least 2-fold (FDR < 0.05) compared to wild-type in any mutant were used for further analysis. Comparison of the differential gene expression profiles of *setdb1 GLKD*

mutant ovaries with *wde* and *hpa1 GLKD* mutant ovaries revealed extensive similarities (Figure 1E). Interestingly, all mutants express an overlapping set of upregulated genes that are not expressed in wild-type ovaries (FPKM <1) (Tables S1-S4; Figures 1F and 1G). Although Gene Ontology (GO) analysis did not identify a biological function associated with these ectopically expressed genes, an examination of the expression data provided by the modENCODE_mRNA-seq_tissues data sets (Brown et al., 2014) reveals that a majority of these ectopically expressed genes are expressed in testis (Figure 1H). In *setdb1 GLKD*, 58% (236/410) are testis-enriched. In *wde GLKD*, 49% (108/220) are testis-enriched, and in *hp1a GLKD*, 52% (170/328) are testis-enriched (Table S4). Moreover, there is a significant overlap between these three data sets (Figure 1I). Together these expression studies suggest that the failure to maintain female identity, as indicated by the depression of testis genes, is a common feature of disrupting H3K9 methylation.

H3K9me3 pathway members control sex-specific transcription at the *phf7* locus

Controlling *phf7* expression is critical for maintaining female germ cell identity (Shapiro-Kulnane et al., 2015). *phf7* transcription is sexually dimorphic. In testis, transcription initiates from an upstream start site giving rise to the *phf7-RC* transcript. In ovaries, the upstream transcription start site (TSS) is not used and transcription initiates at a downstream start site. Visualization of our RNA-seq data aligned to the *Drosophila* genome (UCSC dm6) reveals that the testis-specific *phf7* transcript, *phf7-RC,* is ectopically expressed in *setdb1, wde,* and *hp1a GLKD* mutant ovaries (Figure 2A). Confirmation of these findings by RT-qPCR is presented in Figure 2B.

PHF7 protein expression is limited to male germ cells (Shapiro-Kulnane et al., 2015; Yang et al., 2012). Accordingly, we asked whether the ectopic *phf7-RC* expression observed in mutant ovaries resulted in inappropriate protein expression. To assay for PHF7 protein expression, we used an HA-tagged *phf7* transgene which recapitulates the expected sex-specific protein expression pattern (Figures 2C and 2D) (Shapiro-Kulnane et al., 2015; Yang et al., 2012). In contrast to wild-type ovaries, we find PHF7 protein is detectable in *setdb1, wde,* and *hp1a GLKD* germ cells (Figures 2E 2F and 2G).

Taken together, our results indicate that SETDB1, WDE, and HP1a regulate sex-specific *phf7* transcription, thereby guaranteeing that the male-specific PHF7 protein is not produced.

SETDB1 is required for H3K9me3 enrichment on select protein-encoding genes

Our studies raise the possibility that SETDB1 controls spermatogenesis gene silencing by mediating the deposition of H3K9me3 on its target loci. To test this idea directly, we performed H3K9me3 chromatin immunoprecipitation followed by sequencing (ChIP-seq) on wild-type and *setdb1 GLKD* ovaries. By limiting the differential peak analysis to within 1 kb of euchromatin genes, we identified 746 H3K9me3 enrichment peaks in wild-type that were significantly altered in *setdb1 GLKD* ovaries. Whereas a majority of the gene associated peaks show the expected decrease in H3K9me3 enrichment (84%, 630/746), we also observed regions with an increase in H3K9me3 enrichment (15%, 116/746). How loss of SETDB1 might lead to an increase in H3K9me3 is not known, but we suspect that the effect is indirect.

To identify those genes whose expression is directly affected by SETDB1 in female germ cells, we integrated our ChIP-seq and RNA-seq data sets. These data identify 24 genes which are both ectopically expressed and display a loss of H3K9me3 enrichment in *setdb1 GLKD* mutants (Figure 3A). Previous studies have shown that H3K9me3 is enriched around euchromatic transposable element (TE) insertion sites (Lee, 2015; Lee and Karpen, 2017). This raises the question of whether spermatogenesis gene silencing results from spreading of H3K9me3 from epigenetically silenced transposable elements. However, we observed that only 4 of the 24 silenced genes contained full or partial TE sequences. Therefore, 20 genes are silenced by a SETDB1 mediated mechanism not associated with H3K9me3 spreading from TE insertion sites (Figure 3B). Notably, these genes are not clustered together and the H3K9me3 domains do not spread into the neighboring genes (Figure S2). Moreover, 14 of these genes are testis-enriched, including CG34434 and CG12477 (Figure 3C and 3D). Regional deposition of H3K9me3 is also evident at the *phf7* locus, where H3K9me3 is concentrated over the silenced testis-specific TSS and the intragenic region immediately downstream in wild-type. In

setdb1 GLKD ovaries, where there is testis-specific transcription, a significant reduction in H3K9me3 levels is observed (Figure 4A). Together, these studies identify a set of genes silenced by SETDB1-mediated H3K9 methylation in female germ cells.

SXL promotes H3K9me3 silencing by acting with SETDB1

The distinctive H3K9me3 staining pattern observed in wild-type germ cells is absent in *snf*^{148} mutant germaria (Figure 1B). However, SETDB1 protein remains detectable in *snf*^{148} mutant germ cells (Figure S3). These data, with our finding that SXL protein accumulation is not disrupted in *setdb1 GLKD* germaria (Figure S3), suggests that SXL and SETDB1 are acting in concert to control H3K9me3 deposition. To test this idea we profiled the distribution of H3K9me3 by ChIP-seq in *snf*^{148} mutant ovaries. Differential peak analysis identified changes in H3K9me3 enrichment at 1,039 gene associated peaks in *snf*^{148} mutant ovaries when compared to wild-type. A striking majority of these peaks had decreased enrichment (91%, 948/1039) (Figure 4B). We also observed a small number of regions with increased H3K9me3 levels (9%, 91/1039).

There is a strong overlap between the regions displaying decreased H3K9me3 enrichment in *snf*^{148} and *setdb1 GLKD* mutant ovaries (Figures 4C and 4D). This suggests that SXL and SETDB1 act in concert to promote H3K9me3 silencing of an overlapping set of genes. Indeed, we identify 7 genes (6 in Figure 3B, and *phf7* in Figure 4A) where sex-inappropriate expression is correlated with decreased H3K9me3 enrichment in both *snf*^{148} mutant and *setdb1 GLKD* ovaries. In agreement, analysis of previously published RNA-seq data shows that these genes are inappropriately expressed in *snf*^{148} tumors (Shapiro-Kulnane et al., 2015). Further studies are needed to determine whether repression of one or more of the newly identified co-regulated genes is as important as repression of *phf7* for maintaining female identity.

Discussion

In this study, we identify a previously unknown H3K9me3 epigenetic pathway necessary for sex

maintenance of *Drosophila* ovarian germ cells. In it, *Sxl* is the female specific regulator and SETDB1 is the required chromatin writer. Collectively, our studies support a model in which SETDB1 deposits H3K9me3 repressive marks on its spermatogenesis gene targets, seeding HP1a-dependent silencing without spreading into neighboring loci (Figure 4E). Our studies highlight the emerging importance of H3K9me3 and HP1a deposition, operationally defined as facultative heterochromatin, in maintaining cell fate via stable gene repression (Becker et al., 2016).

An exciting and unexpected implication of our findings is that the sex determination pathway feeds into the heterochromatin pathway. Specifically, we show that the female-specific SXL protein maintains H3K9me3 mediated spermatogenesis silencing. Interestingly, these effects occur without affecting SETDB1 protein expression, suggesting that *Sxl* influences SETDB1 recruitment to specific genomic sites or permit its methylation activity at those sites. A future challenge will be to understand the molecular connection between SXL, a female specific RNA binding protein, and sexually dimorphic epigenetic programming.

phf7 stands out among the genes regulated by facultative heterochromatin because of its pivotal role in controlling germ cell sexual identity (Shapiro-Kulnane et al., 2015; Yang et al., 2012). *phf7* is transcribed in both male and female germ cells with sexually dimorphic transcription start sites. In female germ cells, H3K9me3 decorates the silent testis-specific transcription start site without interfering with transcription from the downstream ovarian transcription start site. Dissolution of the H3K9me3 marks via SXL or SETDB1 knockdown, leads to transcription from the upstream testis-specific site and ectopic protein expression. The only difference between the testis mRNA, which is translated into protein, and the ovary mRNA, which is not, is the length of the 5' UTR. The mechanism that prevents the ovarian mRNA from being translated is unknown. One possible mechanism, suggested by secondary structure analysis, is that the shorter ovarian mRNA forms a stable hairpin loop that inhibits translation. Because non-coding RNAs can function in chromatin regulation (Becker et al., 2016), it is possible that the non-coding ovarian RNA is important for maintaining H3K9me3 silencing of the upstream testis-specific transcription start site. We posit that once the female state of

phf7 expression is initially established, it is perpetuated via an autoregulatory mechanism.

Although the loss of SETDB1 in female germ cells leads to global depression of spermatogenesis genes, our integrative analysis identified only a few genes, in addition to *phf7,* whose misexpression is correlated with a loss of H3K9 methylation. It will be interesting to explore whether any of these genes, like *phf7,* are capable of masculinizing the gene expression program when inappropriately expressed in wild-type female germ cells.

Prior studies have established a role for SETDB1 in germline Piwi-interacting small RNA (piRNA) biogenesis and silencing of transposable elements (TEs) (Rangan et al., 2011; Sienski et al., 2015; Yu et al., 2015). However, piRNAs are unlikely to contribute to sexual identity maintenance. Mutations that specifically interfere with piRNA production, such as *rhino,* do not cause defects in germ cell differentiation (Klattenhoff et al., 2009; Mohn et al., 2014; Volpe et al., 2001; Zhang et al., 2014). Analysis of differential transcription also shows no masculinization of the gene expression program [(Mohn et al., 2014); data not shown]. Thus, the means by which SETDB1 controls spermatogenesis gene silencing is likely to be mechanistically different from what has been described for piRNA-guided H3K9me3 deposition on TEs.

The SETDB1-mediated mechanism for maintaining sexual identity we have uncovered may not be restricted to germ cells. The consequences of switching sexual identity of gut stem cells and somatic gonadal cells also include disruption of tissue homeostasis and tumor formation (Hudry et al., 2016; Ma et al., 2016; 2014; Regan et al., 2016). Furthermore, the loss of HP1a in Drosophila brains leads to masculinization of the neural circuitry and male specific behaviors (Ito et al., 2012). These observations lead us to hypothesize that femaleness is maintained by H3K9me3 silencing of male-specific genes in all tissues.

The conservation of SETDB1 and its role in establishing H3K9me3 mediated silent chromatin suggests that the mechanism for maintaining sexually dimorphic gene expression profiles in Drosophila may be conserved in mammals. Interestingly, H3K9me3 chromatin impedes the reprogramming of somatic cells into pluripotent stem cells (iPSCs). Conversion efficiency is improved by depletion of

SETDB1 (Chen et al., 2013; Soufi et al., 2012; Sridharan et al., 2013). If erasure of H3K9me3 via depletion of SETDB1 alters the sexual identity of the reprogrammed cells, as it does in Drosophila germ cells, the resulting gene expression differences may cause stem cell dysfunction, limiting their therapeutic utility.

Acknowledgments

We thank Jean-Rene Huynh, Mark Van Doren, Prash Rangan, the Bloomington *Drosophila* Stock Center and the Iowa Developmental Studies Hybridoma Bank for fly stocks and antibodies; Alex Miron, Neil Molyneaux, Ricky Chan, Ulrich Ness, Olivia Corradin, Dan Factor, Alina Saiakhova for help with the bioinformatic analysis; Heather Broihier, Michelle Longworth, Ron Conlon, Peter Harte and Peter Scacheri for helpful suggestions, discussions and comments on the manuscript; and Jane Heatwole for fly food. This work was supported by the National Institutes of Health, R01GM102141 to HKS and T32GM008056 to AES. Imaging was performed using equipment purchased through NIH S10OD016164.

Author Contributions

Conceptualization, A.E.S and H.K.S.; Investigation, methodology and analysis A.E.S and L.S.K.; Manuscript writing, reviewing and editing, A.E.S and H.K.S.; Supervision, H.K.S.

Declaration of Interests

The authors declare no competing interests.

Materials and Methods

Contact for reagent and resource sharing

Requests for resources and reagents should be directed to and will be fulfilled by the Lead Contact, Helen Salz (hks@case.edu).

Experimental model and subject details

Fly strains were kept on standard medium at 25^{o}C, except where noted in Methods Details.

Gonads were dissected from adult males and females, 3-5 days post-eclosion, unless otherwise noted. The stocks utilized in this study are listed in the Key Resources Table, and additional information is available on flybase.

Immunofluorescence and image analysis

Drosophila ovaries and testes were fixed and stained according to our previously published procedures (Chau et al., 2009). The following primary antibodies were used: mouse α-spectrin (1:100, Developmental Studies Hybridoma Bank (DSHB), rabbit H3K9me3 (1:1,000, Active Motif), rat HA high affinity (1:500, Roche), and mouse Sxl-M18 (1:100, DSHB). Staining was detected by FITC (1:200,Jackson ImmnoResearch Labs) or Alexa Fluor 555 (1:200,Life Technologies) conjugated species appropriate secondary antibodies. TO-PRO-3 Iodide (Fisher) was used to stain DNA. Images were taken on a Leica SP8 confocal and compiled with Gnu Image Manipulation Program (GIMP) and Microsoft PowerPoint.

RNAi experiments

Knockdown studies were carried out with the following lines generated by the *Drosophila* Transgenic RNAi Project (Hu et al., 2016; Ni et al., 2011; Perkins et al., 2015): *setdb1-P{TRiP.HMS00112}* (BDSC #34803), *Su(var)205/HP1a-P{TRiP.GL00531}* (BDSC #36792), and *wde-P{TRiP.HMS00205}* (BDSC #33339). Different conditions were used to maximize the penetrance of the germ cell tumor phenotype. For knockdown of *setdb1* and *HP1a* the *nos-Gal4;bam-Gal80* driver was used (Matias et al., 2015), crosses were set up at 29°C and adults were aged 3-5 days prior to gonad dissection. For *wde* knockdown the *nos-Gal4* driver was used (BDSC #4937) (Van Doren et al., 1998), crosses were set up at 18°C and adults were transferred to 29°C for 2 days prior to gonad dissection.

qRT-PCR and data analysis

RNA was extracted from dissected ovaries using TRIzol (Invitrogen) and DNase (Promega). Quantity and quality were measured using a NanoDrop spectrophotometer. cDNA was generated by reverse transcription using the SuperScript First-Strand Synthesis System Kit (Invitrogen) using random hexamers. Quantatative real-time PCR was performed using Power SYBR Green PCR Master Mix

(ThermoFisher) with the Applied Biosystems 7300 Real Time PCR system. PCR steps were as follows: 95°C for 10 minutes followed by 40 cycles of 95°C for 15 seconds and 60°C for 1 minute. Melt curves were generated with the following parameters: 95°C for 15 seconds, 60°C for 1 minutes, 95°C for 15 seconds, and 60°C for 15 seconds. Measurements were taken in biological triplicate with two technical replicates. The *phf7-RC* levels were normalized to the total amount *phf7*. Relative transcript amount were calculated using the 2-ΔΔCt method (Livak and Schmittgen, 2001). Primer sequences for measuring the total *phf7* and *phf7-RC* levels are listed in the Key Resources Table.

RNA-seq and data analysis

Total RNA was extracted from dissected ovaries using standard TRIzol (Invitrogen) methods. RNA quality was assessed with Qubit and Agilent Bioanalyzer. Libraries were generated using the Illumina TruSeq Stranded Total RNA kit. Sequencing was completed on 2 biological replicates of each genotype with the Illumina HiSeq 2500 v2 with 100bp paired end reads.

Sequencing reads were aligned to the *Drosophila* genome (UCSC dm6) using TopHat (2.1.0) (Trapnell, 2009). Differential analysis was completed using CuffDiff (2.2.1)(Trapnell et al., 2012). Genes were considering differentially expressed if they exhibited a two-fold or higher change relative to wild-type with a False Discovery Rate (FDR) < 5%. Uniquely expressed genes in mutants had an FPKM < 1 in wild-type ovaries. Testes enriched genes were determined based on modENCODE_mRNA-seq_tissues data sets (Brown et al., 2014). Those genes with an FPKM>1 in testes and <1 in ovaries were considered to be testes enriched. Images were generated using the CummeRbund R package (2.18.0) (Trapnell et al., 2012).

ChIP-seq and data analysis

For each chromatin immunoprecipitation, 400 pairs of *Drosophila* ovaries were dissected in PBS plus protease inhibitors (Roche). Tissues were fixed in 1.8% formaldehyde for 10 minutes at room temperature and quenched with 225 mM glycine for 5 minutes. Tissues were washed twice and stored at -80°C for downstream applications. Samples were lysed using the protocol from Lee et al, 2006. Tissue was placed in lysis buffer 1 (140 mM HEPES pH 7.5, 200 mM NaCl, 1 mM EDTA, 10% glycerol,

0.5% NP-40, 0.25% Triton X-100), homogenized using sterile beads, and rocked at 4°C for 10 minutes. Tissue was then washed 10 minutes at 4°C in lysis buffer 2 (10 mM Tris pH 8, 200 mM NaCl, 1 mM EDTA, 0.5 mM EGTA). Tissues were then placed in 1.5 mL lysis buffer 3 (10 mM Tris pH 8, 100 mM NaCl, 1 mM EDTA, 0.5 mM EGTA, 0.1% Na-deoxycholate, 0.5% N-lauroylsarcosine). All buffers were supplemented with protease inhibitors. Chromatin was sheared to 200-700 base pairs using the QSONICA sonicator (Q800R). The chromatin lysate were incubated overnight at 4°C with H3K9me3 antibodies pre-bound to magnetic beads. The beads were prepared as follows: 25 μl Protein A and 25 μl Protein G Dynabeads per sample were washed twice with ChIP blocking buffer (0.5% Tween 20, 5 mg/mL BSA), then blocked by rocking at 4°C for 1 hour in ChIP blocking buffer, and then conjugated to 5 μg H3K9me3 antibody (abcam) by rocking in new ChIP blocking buffer at 4°C for 1 hour. Following immunoprecipitation, the samples were washed 6 times with ChIP-RIPA buffer (10 mM Tris-HCl pH 8, 1 mM EDTA, 140 mM NaCl, 1% Triton X-100, 0.1% SDS, 0.1% Na-Deoxycholate), 2 times with ChIP-RIPA/500 buffer (ChIP-RIPA + 500 mM NaCl), 2 times with ChIP-LiCl buffer (10 mM Tris-HCl pH 8, 1 mM EDTA, 250 mM LiCl, 0.5% NP-40, 0.5% Na-deoxycholate), and twice with TE buffer. DNA was eluted from beads with 50 μl elution buffer (10 mM Tris-HCl pH 8, 5 mM EDTA, 300 mM NaCl, 0.1% SDS) and reverse crosslinked at 65°C for 6 hours. Beads were spun down and eluted DNA was transferred to a new tube and extracted using phenol-chloroform extraction. All buffers were supplemented with protease inhibitors.

ChIP sequencing libraries were prepared using the Rubicon Genomics Library Prep Kit with 16 amplification cycles. DNA was cleaned and assessed for quality with Qubit and Agilent Bioanalyzer. Sequencing was completed on 2 biological replicates of each genotype with the Illumina HiSeq 2500 v2 with 50 bp single end reads.

H3K9me3 reads were aligned to the *Drosophila* genome (UCSC dm6) using bowtie2 (2.2.6) (Langmead and Salzberg, 2012), and duplicate reads were removed with samtools (1.3) (Li et al., 2009). Peaks were called with MACS (2.1.20150731) using the broadpeaks option with all other

paramaters set to default (Zhang et al., 2008). Differential peak analysis on all replicates was completed with the DIFFBIND program (2.4.8), using summits=500 and the DESeq2 package http://bioconductor.org/packages/release/bioc/vignettes/DiffBind/inst/doc/DiffBind.pdf. The mean peak concentration was calculated by normalizing reads to the total library size and subtracting the corresponding input reads. Differential peak fold changes were calculated by subtracting wild-type mean concentrations from mutant mean concentrations. Mutant peaks were considered significantly altered relative to wild-type if they had a False Discovery Rate (FDR) < 5%.

The average H3K9me3 deposition on genes in wild-type ovaries was generated with deeptools (2.5.3), using normalized ChIP reads from wild-type ovaries (Ramirez et al., 2016).

Data availability

RNA-seq and ChIP-seq data sets are available from the National Center for Biotechnology Information's GEO database (http://www.ncbi.nlm.nih.gov/geo/) under accession number GSE109852.

References

Becker, J.S., Nicetto, D., Zaret, K.S., 2016. H3K9me3-Dependent Heterochromatin: Barrier to Cell Fate Changes. Trends Genet. 32, 29–41. doi:10.1016/j.tig.2015.11.001

Brower-Toland, B., Riddle, N.C., Jiang, H., Huisinga, K.L., Elgin, S.C.R., 2009. Multiple SET methyltransferases are required to maintain normal heterochromatin domains in the genome of Drosophila melanogaster. Genetics 181, 1303–1319. doi:10.1534/genetics.108.100271

Brown, J.B., Boley, N., Eisman, R., May, G.E., Stoiber, M.H., Duff, M.O., Booth, B.W., Wen, J., Park, S., Suzuki, A.M., Wan, K.H., Yu, C., Zhang, D., Carlson, J.W., Cherbas, L., Eads, B.D., Miller, D., Mockaitis, K., Roberts, J., Davis, C.A., Frise, E., Hammonds, A.S., Olson, S., Shenker, S., Sturgill, D., Samsonova, A.A., Weiszmann, R., Robinson, G., Hernandez, J., Andrews, J., Bickel, P.J., Carninci, P., Cherbas, P., Gingeras, T.R., Hoskins, R.A., Kaufman, T.C., Lai, E.C., Oliver, B., Perrimon, N., Graveley, B.R., Celniker, S.E., 2014. Diversity and dynamics of the Drosophila transcriptome. Nature 512, 393–399. doi:10.1038/nature12962

Casper, A.L., Van Doren, M., 2009. The establishment of sexual identity in the Drosophila germline. Development 136, 3821–3830. doi:10.1242/dev.042374

Chau, J., Kulnane, L.S., Salz, H.K., 2012. Sex-lethal enables germline stem cell differentiation by down-regulating Nanos protein levels during Drosophila oogenesis. Proc. Natl. Acad. Sci. U.S.A. 109, 9465–9470. doi:10.1073/pnas.1120473109

Chau, J., Kulnane, L.S., Salz, H.K., 2009. Sex-lethal facilitates the transition from germline stem cell to committed daughter cell in the Drosophila ovary. Genetics 182, 121–132. doi:10.1534/genetics.109.100693

Chen, J., Liu, H., Liu, J., Qi, J., Wei, B., Yang, J., Liang, H., Chen, Y., Chen, J., Wu, Y., Guo, L., Zhu, J., Zhao, X., Peng, T., Zhang, Y., Chen, S., Li, X., Li, D., Wang, T., Pei, D., 2013. H3K9 methylation is

a barrier during somatic cell reprogramming into iPSCs. Nat. Genet. 45, 34–42. doi:10.1038/ng.2491

Clough, E., Moon, W., Wang, S., Smith, K., Hazelrigg, T., 2007. Histone methylation is required for oogenesis in Drosophila. Development 134, 157–165. doi:10.1242/dev.02698

Eissenberg, J.C., Elgin, S.C.R., 2014. HP1a: a structural chromosomal protein regulating transcription. Trends Genet. 30, 103–110. doi:10.1016/j.tig.2014.01.002

Elgin, S.C.R., Reuter, G., 2013. Position-effect variegation, heterochromatin formation, and gene silencing in Drosophila. Cold Spring Harbor Perspectives in Biology 5, a017780–a017780. doi:10.1101/cshperspect.a017780

Horabin, J.I., Bopp, D., Waterbury, J., Schedl, P., 1995. Selection and maintenance of sexual identity in the Drosophila germline. Genetics 141, 1521–1535.

Hu, Y., Comjean, A., Roesel, C., Vinayagam, A., Flockhart, I., Zirin, J., Perkins, L., Perrimon, N., Mohr, S.E., 2016. FlyRNAi.org-the database of the Drosophila RNAi screening center and transgenic RNAi project: 2017 update. Nucleic Acids Res. doi:10.1093/nar/gkw977

Hudry, B., Khadayate, S., Miguel-Aliaga, I., 2016. The sexual identity of adult intestinal stem cells controls organ size and plasticity. Nature 530, 344–348. doi:10.1038/nature16953

Ito, H., Sato, K., Koganezawa, M., Ote, M., Matsumoto, K., Hama, C., Yamamoto, D., 2012. Fruitless recruits two antagonistic chromatin factors to establish single-neuron sexual dimorphism. Cell 149, 1327–1338. doi:10.1016/j.cell.2012.04.025

Klattenhoff, C., Xi, H., Li, C., Lee, S., Xu, J., Khurana, J.S., Zhang, F., Schultz, N., Koppetsch, B.S., Nowosielska, A., Seitz, H., Zamore, P.D., Weng, Z., Theurkauf, W.E., 2009. The Drosophila HP1 homolog Rhino is required for transposon silencing and piRNA production by dual-strand clusters. Cell 138, 1137–1149. doi:10.1016/j.cell.2009.07.014

Koch, C.M., Honemann-Capito, M., Egger-Adam, D., Wodarz, A., 2009. Windei, the Drosophila homolog of mAM/MCAF1, is an essential cofactor of the H3K9 methyl transferase dSETDB1/Eggless in germ line development. PLoS Genet 5, e1000644. doi:10.1371/journal.pgen.1000644

Langmead, B., Salzberg, S.L., 2012. Fast gapped-read alignment with Bowtie 2. Nat. Methods 9, 357–359. doi:10.1038/nmeth.1923

Lee, Y.C.G., 2015. The Role of piRNA-Mediated Epigenetic Silencing in the Population Dynamics of Transposable Elements in Drosophila melanogaster. PLoS Genet 11, e1005269. doi:10.1371/journal.pgen.1005269

Lee, Y.C.G., Karpen, G.H., 2017. Pervasive epigenetic effects of Drosophila euchromatic transposable elements impact their evolution. Elife 6, 2185. doi:10.7554/eLife.25762

Lesch, B.J., Page, D.C., 2012. Genetics of germ cell development. Nature Reviews Genetics 13, 781–794. doi:10.1038/nrg3294

Li, H., Handsaker, B., Wysoker, A., Fennell, T., Ruan, J., Homer, N., Marth, G., Abecasis, G., Durbin, R., 1000 Genome Project Data Processing Subgroup, 2009. The Sequence Alignment/Map format and SAMtools. Bioinformatics 25, 2078–2079. doi:10.1093/bioinformatics/btp352

Livak, K.J., Schmittgen, T.D., 2001. Analysis of relative gene expression data using real-time quantitative PCR and the 2(-Delta Delta C(T)) Method. Methods 25, 402–408. doi:10.1006/meth.2001.1262

Ma, Q., de Cuevas, M., Matunis, E.L., 2016. Chinmo is sufficient to induce male fate in somatic cells of

the adult Drosophila ovary. Development. doi:10.1242/dev.129627

Ma, Q., Wawersik, M., Matunis, E.L., 2014. The Jak-STAT Target Chinmo Prevents Sex Transformation of Adult Stem Cells in the Drosophila Testis Niche. Dev Cell 31, 474–486. doi:10.1016/j.devcel.2014.10.004

Matias, N.R., Mathieu, J., Huynh, J.-R., 2015. Abscission is regulated by the ESCRT-III protein shrub in Drosophila germline stem cells. PLoS Genet 11, e1004653. doi:10.1371/journal.pgen.1004653

Mohn, F., Sienski, G., Handler, D., Brennecke, J., 2014. The rhino-deadlock-cutoff complex licenses noncanonical transcription of dual-strand piRNA clusters in Drosophila. Cell 157, 1364–1379. doi:10.1016/j.cell.2014.04.031

Nagengast, A.A., Stitzinger, S.M., Tseng, C.-H., Mount, S.M., Salz, H.K., 2003. Sex-lethal splicing autoregulation in vivo: interactions between SEX-LETHAL, the U1 snRNP and U2AF underlie male exon skipping. Development 130, 463–471.

Ni, J.-Q., Zhou, R., Czech, B., Liu, L.-P., Holderbaum, L., Yang-Zhou, D., Shim, H.-S., Tao, R., Handler, D., Karpowicz, P., Binari, R., Booker, M., Brennecke, J., Perkins, L.A., Hannon, G.J., Perrimon, N., 2011. A genome-scale shRNA resource for transgenic RNAi in Drosophila. Nat. Methods 8, 405–407. doi:10.1038/nmeth.1592

Perkins, L.A., Holderbaum, L., Tao, R., Hu, Y., Sopko, R., McCall, K., Yang-Zhou, D., Flockhart, I., Binari, R., Shim, H.-S., Miller, A., Housden, A., Foos, M., Randkelv, S., Kelley, C., Namgyal, P., Villalta, C., Liu, L.-P., Jiang, X., Huan-Huan, Q., Wang, X., Fujiyama, A., Toyoda, A., Ayers, K., Blum, A., Czech, B., Neumuller, R., Yan, D., Cavallaro, A., Hibbard, K., Hall, D., Cooley, L., Hannon, G.J., Lehmann, R., Parks, A., Mohr, S.E., Ueda, R., Kondo, S., Ni, J.-Q., Perrimon, N., 2015. The Transgenic RNAi Project at Harvard Medical School: Resources and Validation. Genetics 201, 843–852. doi:10.1534/genetics.115.180208

Ramirez, F., Ryan, D.P., Gruning, B., Bhardwaj, V., Kilpert, F., Richter, A.S., Heyne, S., Dundar, F., Manke, T., 2016. deepTools2: a next generation web server for deep-sequencing data analysis. Nucleic Acids Res 44, W160–5. doi:10.1093/nar/gkw257

Rangan, P., Malone, C.D., Navarro, C., Newbold, S.P., Hayes, P.S., Sachidanandam, R., Hannon, G.J., Lehmann, R., 2011. piRNA production requires heterochromatin formation in Drosophila. Curr Biol 21, 1373–1379. doi:10.1016/j.cub.2011.06.057

Regan, J.C., Khericha, M., Dobson, A.J., Bolukbasi, E., Rattanavirotkul, N., Partridge, L., 2016. Sex difference in pathology of the ageing gut mediates the greater response of female lifespan to dietary restriction. Elife 5. doi:10.7554/eLife.10956

Salz, H.K., Dawson, E.P., Heaney, J.D., 2017. Germ cell tumors: Insights from the Drosophila ovary and the mouse testis. Mol. Reprod. Dev. 84, 200–211. doi:10.1002/mrd.22779

Schüpbach, T., 1985. Normal female germ cell differentiation requires the female X chromosome to autosome ratio and expression of sex-lethal in Drosophila melanogaster. Genetics 109, 529–548.

Shapiro-Kulnane, L., Smolko, A.E., Salz, H.K., 2015. Maintenance of Drosophila germline stem cell sexual identity in oogenesis and tumorigenesis. Development 142, 1073–1082. doi:10.1242/dev.116590

Sienski, G., Batki, J., Senti, K.-A., Dönertas, D., Tirian, L., Meixner, K., Brennecke, J., 2015. Silencio/CG9754 connects the Piwi-piRNA complex to the cellular heterochromatin machinery. Genes Dev 29, 2258–2271. doi:10.1101/gad.271908.115

Soufi, A., Donahue, G., Zaret, K.S., 2012. Facilitators and impediments of the pluripotency reprogramming factors' initial engagement with the genome. Cell 151, 994–1004.

doi:10.1016/j.cell.2012.09.045

Spiller, C., Koopman, P., Bowles, J., 2017. Sex Determination in the Mammalian Germline. Annu. Rev. Genet. 51, 265–285. doi:10.1146/annurev-genet-120215-035449

Sridharan, R., Gonzales-Cope, M., Chronis, C., Bonora, G., McKee, R., Huang, C., Patel, S., Lopez, D., Mishra, N., Pellegrini, M., Carey, M., Garcia, B.A., Plath, K., 2013. Proteomic and genomic approaches reveal critical functions of H3K9 methylation and heterochromatin protein-1γ in reprogramming to pluripotency. Nat Cell Biol 15, 872–882. doi:10.1038/ncb2768

Staab, S., Heller, A., Steinmann-Zwicky, M., 1996. Somatic sex-determining signals act on XX germ cells in Drosophila embryos. Development 122, 4065–4071.

Timms, R.T., Tchasovnikarova, I.A., Antrobus, R., Dougan, G., Lehner, P.J., 2016. ATF7IP-Mediated Stabilization of the Histone Methyltransferase SETDB1 Is Essential for Heterochromatin Formation by the HUSH Complex. CellReports 17, 653–659. doi:10.1016/j.celrep.2016.09.050

Trapnell, C., Roberts, A., Goff, L., Pertea, G., Kim, D., Kelley, D.R., Pimentel, H., Salzberg, S.L., Rinn, J.L., Pachter, L., 2012. Differential gene and transcript expression analysis of RNA-seq experiments with TopHat and Cufflinks. Nat Protoc 7, 562–578. doi:10.1038/nprot.2012.016

Van Doren, M., Williamson, A.L., Lehmann, R., 1998. Regulation of zygotic gene expression in Drosophila primordial germ cells. Curr Biol 8, 243–246.

Volpe, A.M., Horowitz, H., Grafer, C.M., Jackson, S.M., Berg, C.A., 2001. Drosophila rhino encodes a female-specific chromo-domain protein that affects chromosome structure and egg polarity. Genetics 159, 1117–1134.

Wang, X., Pan, L., Wang, S., Zhou, J., McDowell, W., Park, J., Haug, J., Staehling, K., Tang, H., Xie, T., 2011. Histone H3K9 trimethylase Eggless controls germline stem cell maintenance and differentiation. PLoS Genet 7, e1002426–e1002426. doi:10.1371/journal.pgen.1002426

Wawersik, M., Milutinovich, A., Casper, A.L., Matunis, E., Williams, B., Van Doren, M., 2005. Somatic control of germline sexual development is mediated by the JAK/STAT pathway. Nature 436, 563–567. doi:10.1038/nature03849

Yang, S.Y., Baxter, E.M., Van Doren, M., 2012. Phf7 controls male sex determination in the Drosophila germline. Dev Cell 22, 1041–1051. doi:10.1016/j.devcel.2012.04.013

Yoon, J., Lee, K.-S., Park, J.S., Yu, K., Paik, S.-G., Kang, Y.-K., 2008. dSETDB1 and SU(VAR)3-9 sequentially function during germline-stem cell differentiation in Drosophila melanogaster. PLoS ONE 3, e2234–e2234. doi:10.1371/journal.pone.0002234

Yu, Y., Gu, J., Jin, Y., Luo, Y., Preall, J.B., Ma, J., Czech, B., Hannon, G.J., 2015. Panoramix enforces piRNA-dependent cotranscriptional silencing. Science 350, 339–342. doi:10.1126/science.aab0700

Zhang, Y., Liu, T., Meyer, C.A., Eeckhoute, J., Johnson, D.S., Bernstein, B.E., Nusbaum, C., Myers, R.M., Brown, M., Li, W., Liu, X.S., 2008. Model-based analysis of ChIP-Seq (MACS). Genome Biol 9, R137. doi:10.1186/gb-2008-9-9-r137

Zhang, Z., Wang, J., Schultz, N., Zhang, F., Parhad, S.S., Tu, S., Vreven, T., Zamore, P.D., Weng, Z., Theurkauf, W.E., 2014. The HP1 homolog rhino anchors a nuclear complex that suppresses piRNA precursor splicing. Cell 157, 1353–1363. doi:10.1016/j.cell.2014.04.030

Figure Legends

Figure 1. Loss of H3K9me3 leads to ectopic spermatogenesis gene expression

(A-D) Representative confocal images of a wild-type (WT), *snf*^{148}*, setdb1 GLKD, and wde GLKD* germarium stained for H3K9me3. In B-D, germaria are outlined by dashed white lines. Scale bar, 25 μm. (E) Heat map comparing changes in gene expression in *setdb1, wde,* and *hp1a GLKD* ovaries compared to wild-type ovaries. Each row depicts a gene with significantly altered expression in at least one mutant. (F) Heat map comparing ectopically expressed genes in *setdb1, wde,* and *hp1a GLKD* ovaries (FPKM < 1 in wild-type ovaries). Each row depicts a gene that is ectopically expressed in at least one mutant. (G) Venn diagram showing overlap of ectopically expressed genes in *setdb1, wde,* and *hp1a GLKD* ovaries. (H) Bar chart showing the percentage of ectopically expressed genes in *setdb1, wde,* and *hp1a GLKD* ovaries that are expressed in wild-type testis (testis enriched). (I) Venn diagram showing the overlap of ectopically expressed spermatogenesis genes in *setdb1, wde,* and *hp1a GLKD* ovaries.

Figure 2. SETDB1, WDE, and HP1a depletion leads to female-to-male reprogramming at the *phf7* locus

(A) Genome browser view of the *phf7* locus. Tracks show RNA-seq reads aligned to the *Drosophila* genome (UCSC dm6). All tracks are viewed at the same scale. The screen shot is reversed so that the 5' end of the gene is on the left. The reads that are unique to the mutant *GLKD* ovaries are highlighted by gray shading. Beneath is the RefSeq gene annotation are the two *phf7* transcripts, *phf7-RC* and *phf7-RA*. Transcription start sites are indicated by blue (*phf7-RC)* and pink (*phf7-RA)* arrows. Primers for RT-qPCR are indicated by arrowheads: gray for *phf7-RC,* red for total *phf7.* (B) RT-qPCR analysis of the *phf7-RC* transcript in wild-type testis, wild-type ovaries, *setdb1, wde,* and *hp1a GLKD* ovaries. Expression, normalized to the total level of *phf7*, is shown as fold change relative to testis. Error bars indicate SD of three biological replicates. (C) Representative confocal images of the tip of a wild-type

testis and (D-G) germaria from wild-type and *setdb1, wde,* and *hp1a GLKD* animals carrying a copy of an HA-*phf7* transgene stained for HA (green) and DNA (red). Scale bar, 25 μm.

Figure 3. Loss of SETDB1 in female germ cells leads to H3K9me3 depletion on select protein-encoding genes

(A) Scatter plot showing the significantly altered (FDR < 5%) H3K9me3 peaks in *setdb1 GLKD* ovaries relative to wild-type (WT) ovaries. Negative values indicate a reduction in H3K9me3 in mutant ovaries. Reduced peaks associated with ectopically expressed genes are labeled in red. (B) List of 20 genes which are both ectopically expressed and display a loss of H3K9me3 enrichment in *setdb1 GLKD* ovaries. Genes in bold are also ectopically expressed and display a loss of H3K9me3 enrichment in snf^{148} mutant ovaries. (C-D) Genome browser view of the *CG34434, and CG12477* loci. H3K9me3 and RNA reads in wild-type (WT) and *setdb1 GLKD* are shown. The screen shots are reversed so the 5' end is on the left. Boxes indicate the gene locus of interest.

Figure 4. Loss of SXL interferes with H3K9me3 accumulation on select protein-encoding genes

(A) Genome browser view of the *phf7* locus. Tracks show H3K9me3 reads aligned to the *Drosophila* genome (UCSC dm6). All tracks are viewed at the same scale. The screen shot is reversed so that the 5' end of the gene is on the left. Beneath is the RefSeq gene annotation of the two *phf7* transcripts, *phf7-RC* and *phf7-RA*. Transcription start sites are indicated by blue (*phf7-RC)* and pink (*phf7-RA)* arrows. (B) Scatter plot of significantly altered (FDR < 5%) H3K9me3 peaks in snf^{148} ovaries relative to wild-type (WT) ovaries. Negative values indicate a decreased H3K9me3 peak in mutant ovaries. (C) Heat map comparing the differential H3K9me3 peak analysis carried out in snf^{148} and *setdb1 GLKD* ovaries Each row depicts a gene with a significantly altered peak in either snf^{148} or *setdb1 GLKD* ovaries compared to wild-type. (D) Plot comparing the significantly altered H3K9me3 peaks observed in snf^{148} ovaries to *setdb1 GLKD* ovaries. Genes ectopically expressed in *setdb1 GLKD* are labeled in red while those that are ectopically expressed and testes enriched are labeled in blue. (E) Model. In wild-

type germ cells, SXL acts in concert with SETDB1 to establish repressive H3K9me3/HP1a domains on select spermatogenesis genes.

Supplemental Information

Figure S1. (Related to Figure 1) H3K9me3 is required for germ cell differentiation

(A, B) Representative confocal images of a wild-type and *setdb1 GLKD* germarium stained for DNA (red) and α-spectrin (green) to visualize spectrosomes (sp), fusomes (fu) and somatic cells Scale bar, 25 μm. (C) Quantification of the number of round spectrosome-like structures per germarium in wild-type, *wde GLKD, hp1a GLKD,* and *setdb1 GLKD* backgrounds. The number of germaria counted is shown above each bar.

Figure S2. (Related to Figure 3) H3K9me3 peaks on genes ectopically expressed in *setdb1 GLKD* ovaries do not spread to neighboring genes, and are not clustered together in the genome.

(A) The average H3K9me3 enrichment profile near open reading frames, scaled to 1500 base pairs, ± 3 kb. In light blue, the average enrichment profile of genes which display an H3K9me3 peak in wild-type ovaries. In dark blue, the average profile of genes which display a loss of H3K9me3 enrichment in *setdb1 GLKD* ovaries. In yellow, the average profile of genes which are both ectopically expressed and display a loss of H3K9me3 enrichment in *setdb1 GLKD* ovaries. (B) The genomic locations of the 20 genes which are both ectopically expressed and display a loss of H3K9me3 enrichment in *setdb1 GLKD* ovaries.

Figure S3. (Related to Figure 4) SETDB1 does not regulate SXL protein expression and SXL does not regulate SETDB1 protein expression.

(A, B) Representative confocal images of a wild-type (WT) and *setdb1 GLKD* germarium stained for DNA (red) and SXL (green). Scale bar, 25 μm. (C, D) Representative confocal images of a germaria from wild-type and snf^{148} females carrying a copy an endogenously HA-tagged allele of *setdb1* stained for HA. Scale bar, 12.5 μm.

Table S1 (Related to Figure 1). Genes upregulated at least 2-fold in *setdb1 GLKD* ovaries.

Table S2 (Related to Figure 1). Genes upregulated at least 2-fold in *wde GLKD* ovaries.

Table S3 (Related to Figure 1). Genes upregulated at least 2-fold in *hp1a GLKD* ovaries.

Table S4 (Related to Figure 1). List of genes ectopically expressed in *setdb1 GLKD, wde GLKD* and *hp1a GLKD* ovaries.

Figure 1

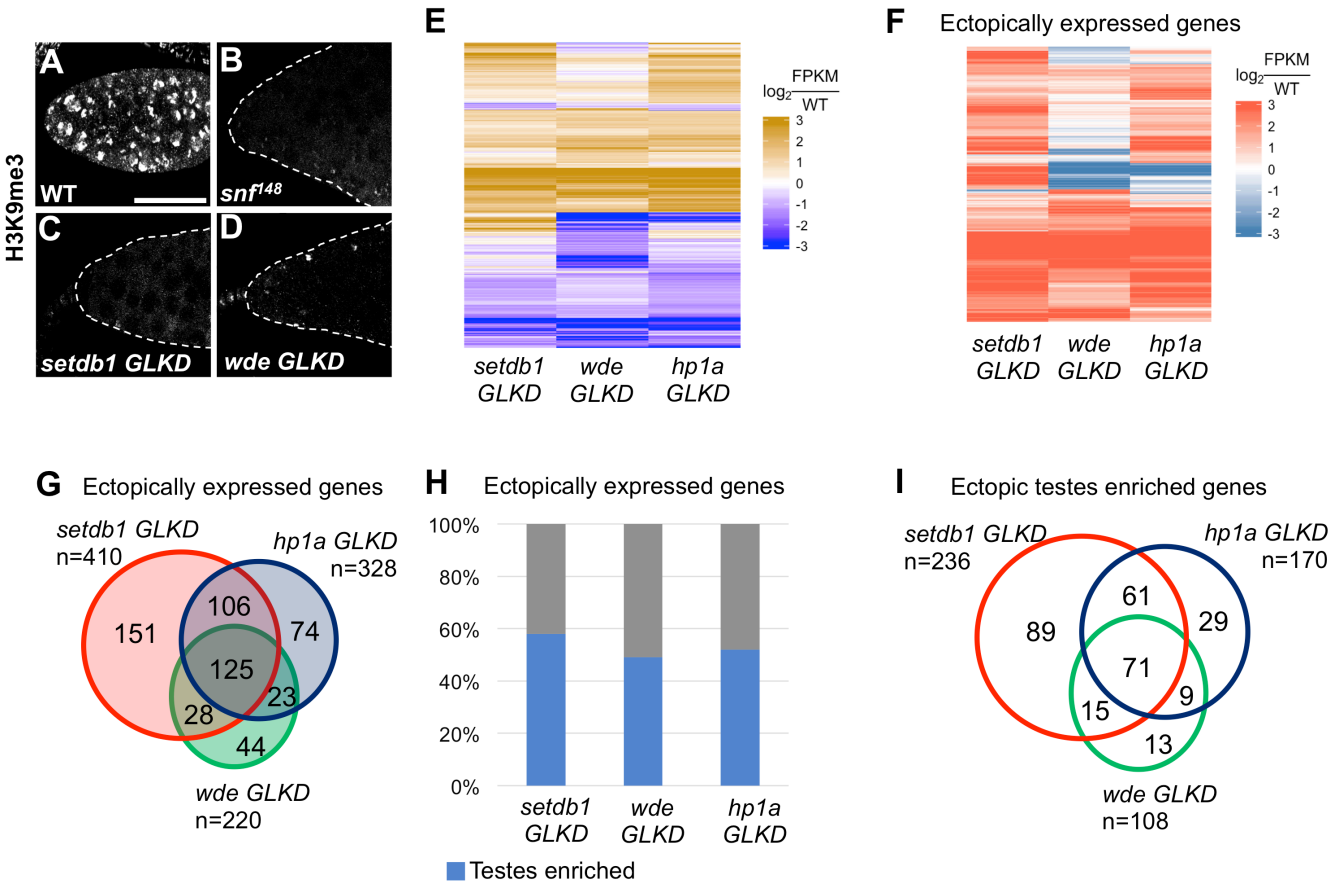

Figure 1. Loss of H3K9me3 leads to ectopic spermatogenesis gene expression
(A-D) Representative confocal images of a wild-type (WT), *snf*^{148}*, setdb1 GLKD, and wde GLKD* germarium stained for H3K9me3. In B-D, germaria are outlined by dashed white lines. Scale bar, 25 μm. (E) Heat map comparing changes in gene expression in *setdb1, wde,* and *hp1a GLKD* ovaries compared to wild-type ovaries. Each row depicts a gene with significantly altered expression in at least one mutant. (F) Heat map comparing ectopically expressed genes in *setdb1, wde,* and *hp1a GLKD* ovaries (FPKM < 1 in wild-type ovaries). Each row depicts a gene that is ectopically expressed in at least one mutant. (G) Venn diagram showing overlap of ectopically expressed genes in *setdb1, wde,* and *hp1a GLKD* ovaries. (H) Bar chart showing the percentage of ectopically expressed genes in *setdb1, wde,* and *hp1a GLKD* ovaries that are expressed in wild-type testis (testis enriched). (I) Venn diagram showing the overlap of ectopically expressed spermatogenesis genes in *setdb1, wde,* and *hp1a GLKD* ovaries.

Figure 2

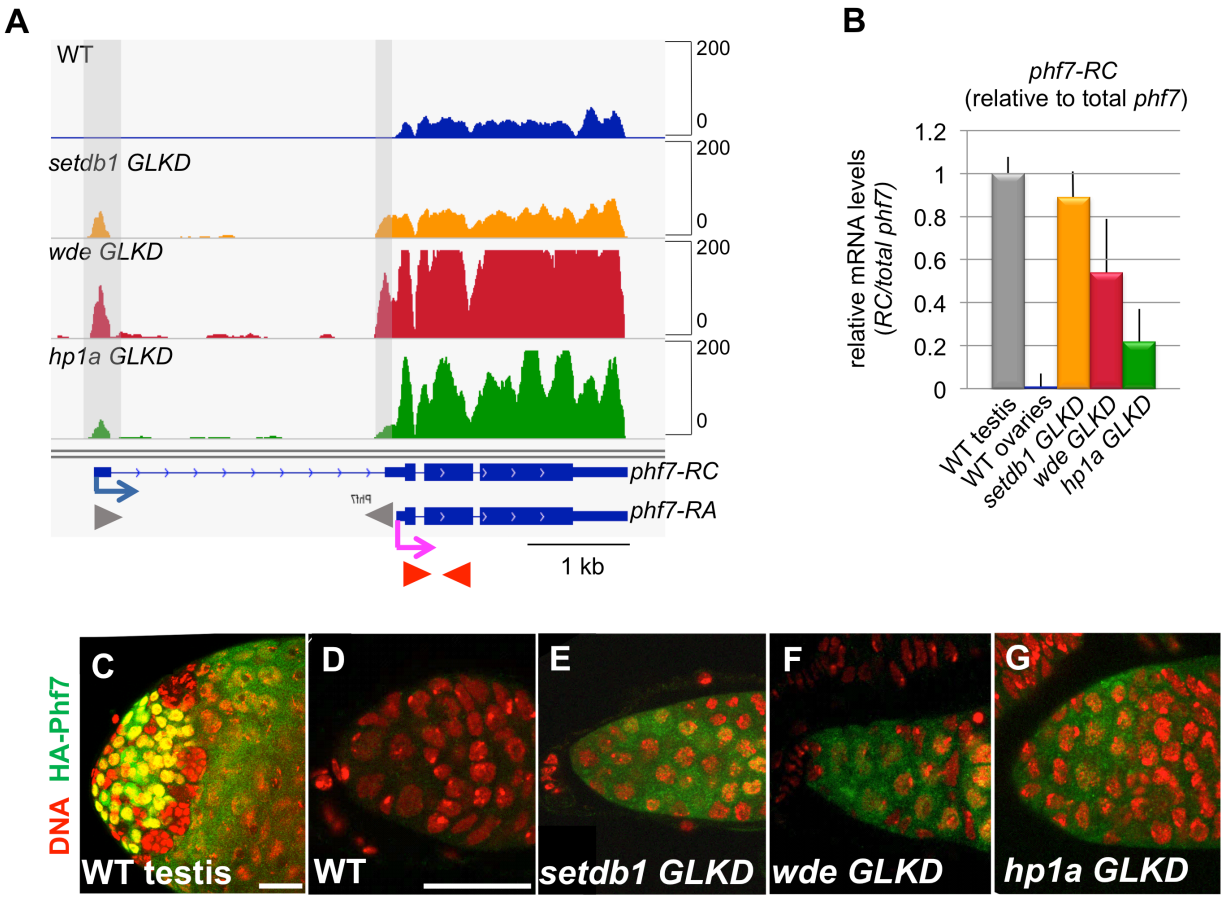

Figure 2. SETDB1, WDE, and HP1a depletion leads to female-to-male reprogramming at the *phf7* locus

(A) Genome browser view of the *phf7* locus. Tracks show RNA-seq reads aligned to the *Drosophila* genome (UCSC dm6). All tracks are viewed at the same scale. The screen shot is reversed so that the 5' end of the gene is on the left. The reads that are unique to the mutant *GLKD* ovaries are highlighted by gray shading. Beneath is the RefSeq gene annotation are the two *phf7* transcripts, *phf7-RC* and *phf7-RA*. Transcription start sites are indicated by blue (*phf7-RC)* and pink (*phf7-RA)* arrows. Primers for RT-qPCR are indicated by arrowheads: gray for *phf7-RC,* red for total *phf7.* (B) RT-qPCR analysis of the *phf7-RC* transcript in wild-type testis, wild-type ovaries, *setdb1, wde,* and *hp1a GLKD* ovaries. Expression, normalized to the total level of *phf7*, is shown as fold change relative to testis. Error bars indicate SD of three biological replicates. (C) Representative confocal images of the tip of a wild-type testis and (D-G) germaria from wild-type and *setdb1, wde,* and *hp1a GLKD* animals carrying a copy of an HA-*phf7* transgene stained for HA (green) and DNA (red). Scale bar, 25 μm.

A

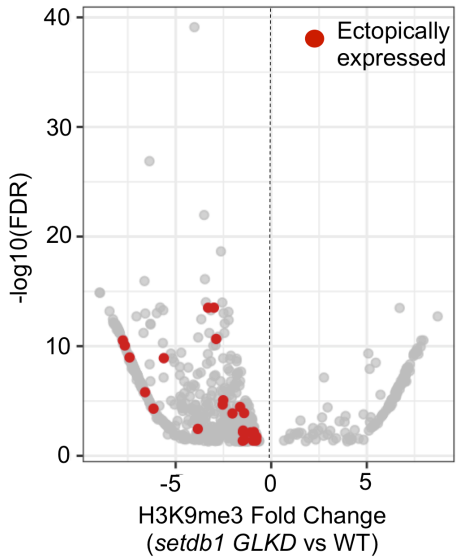

B

Gene	Protein domain, group membership and/or predicted molecular function	Testis enriched
CG10440	BTB/POZ domain	YES
CG10483	SPX and EXS domains	YES
CG12061	Sodium/calcium exchanger	YES
CG12477	**Zinc finger**	**YES**
CG13423	Peptidase	YES
CG15172	**Unknown**	**YES**
CG17636	Hydrolase	YES
CG32506	GTPase	YES
CG34434	**Unknown**	**YES**
CG42299	**Zinc finger**	**YES**
CG42613	Peptidase	YES
CR43299	ncRNA	YES
Lim1	Homeobox DNA binding	YES
skpE	**Ubiquitin transferase**	**YES**
CG12607	Unknown	NO
CG15818	Carbohydrate binding	NO
CG31202	Calcium binding	NO
CG32679	Secretory protein	NO
MsR1	GPCR signaling	NO
Rab3-GEF	**Nucleotide exchange factor**	**NO**

C

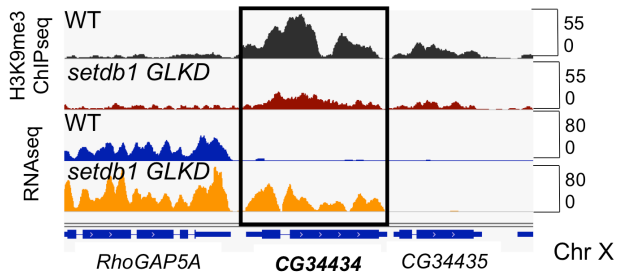

D

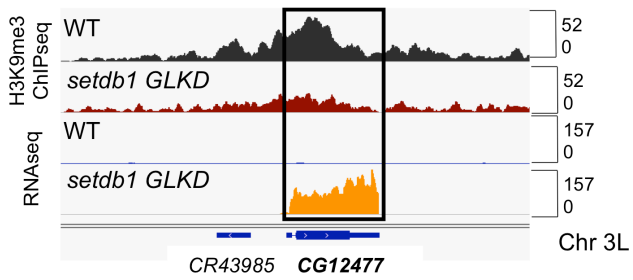

Figure 3. Loss of SETDB1 in female germ cells leads to H3K9me3 depletion on select protein-encoding genes

(A) Scatter plot showing the significantly altered (FDR < 5%) H3K9me3 peaks in *setdb1 GLKD* ovaries relative to wild-type (WT) ovaries. Negative values indicate a reduction in H3K9me3 in mutant ovaries. Reduced peaks associated with ectopically expressed genes are labeled in red. (B) List of 20 genes which are both ectopically expressed and display a loss of H3K9me3 enrichment in *setdb1 GLKD* ovaries. Genes in bold are also ectopically expressed and display a loss of H3K9me3 enrichment in *snf*^{148} mutant ovaries. (C-D) Genome browser view of the *CG34434, and CG12477* loci. H3K9me3 and RNA reads in wild-type (WT) and *setdb1 GLKD* are shown. The screen shots are reversed so the 5' end is on the left. Boxes indicate the gene locus of interest.

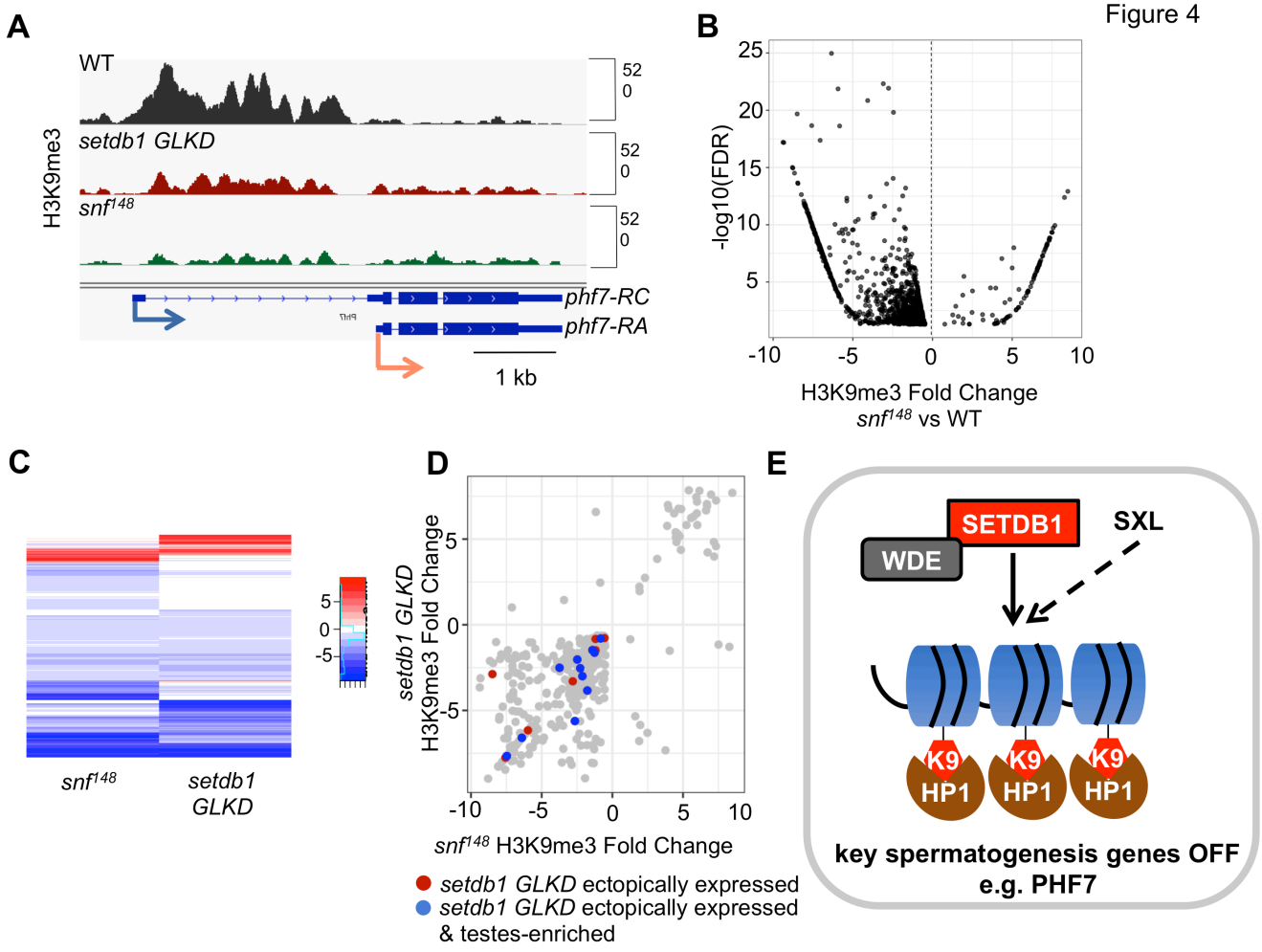

Figure 4. Loss of SXL interferes with H3K9me3 accumulation on select protein-encoding genes
(A) Genome browser view of the *phf7* locus. Tracks show H3K9me3 reads aligned to the *Drosophila* genome (UCSC dm6). All tracks are viewed at the same scale. The screen shot is reversed so that the 5' end of the gene is on the left. Beneath is the RefSeq gene annotation of the two *phf7* transcripts, *phf7-RC* and *phf7-RA*. Transcription start sites are indicated by blue (*phf7-RC)* and pink (*phf7-RA)* arrows. (B) Scatter plot of significantly altered (FDR < 5%) H3K9me3 peaks in *snf*^{148} ovaries relative to wild-type (WT) ovaries. Negative values indicate a decreased H3K9me3 peak in mutant ovaries. (C) Heat map comparing the differential H3K9me3 peak analysis carried out in *snf*^{148} and *setdb1 GLKD* ovaries Each row depicts a gene with a significantly altered peak in either *snf*^{148} or *setdb1 GLKD* ovaries compared to wild-type. (D) Plot comparing the significantly altered H3K9me3 peaks observed in *snf*^{148} ovaries to *setdb1 GLKD* ovaries. Genes ectopically expressed in *setdb1 GLKD* are labeled in red while those that are ectopically expressed and testes enriched are labeled in blue. (E) Model. In wild-type germ cells, SXL acts in concert with SETDB1 to establish repressive H3K9me3/HP1a domains on select spermatogenesis genes.

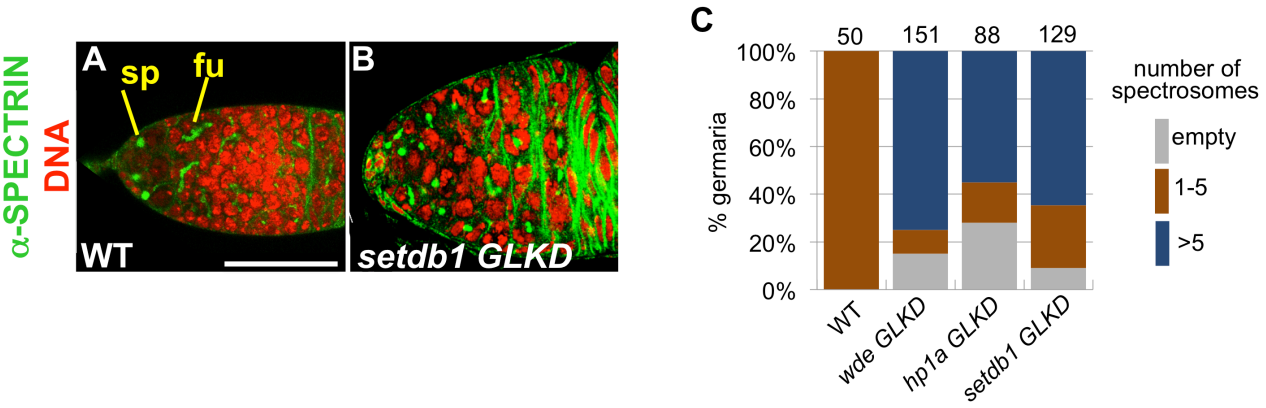

Figure S1. (Related to Figure 1) H3K9me3 is required for germ cell differentiation
(A, B) Representative confocal images of a wild-type and *setdb1 GLKD* germarium stained for DNA (red) and α-spectrin (green) to visualize spectrosomes (sp), fusomes (fu) and somatic cells Scale bar, 25 μm. (C) Quantification of the number of round spectrosome-like structures per germarium in wild-type, *wde GLKD, hp1a GLKD,* and *setdb1 GLKD* backgrounds. The number of germaria counted is shown above each bar.

Figure S2

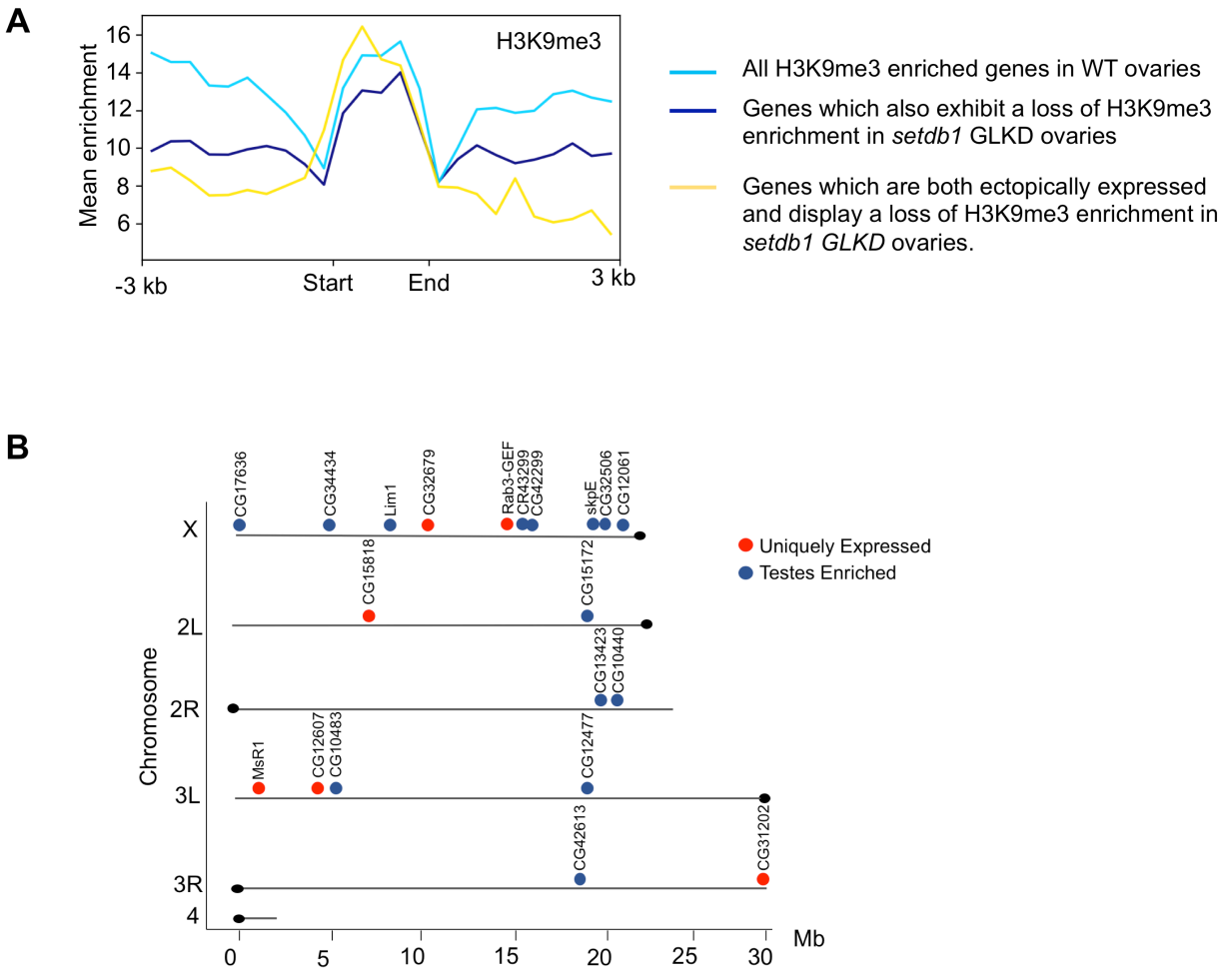

Figure S2. (Related to Figure 3) H3K9me3 peaks on genes ectopically expressed in *setdb1 GLKD* ovaries do not spread to neighboring genes, and are not clustered together in the genome.

(A) The average H3K9me3 enrichment profile near open reading frames, scaled to 1500 base pairs, ± 3 kb. In light blue, the average enrichment profile of genes which display an H3K9me3 peak in wild-type ovaries. In dark blue, the average profile of genes which display a loss of H3K9me3 enrichment in *setdb1 GLKD* ovaries. In yellow, the average profile of genes which are both ectopically expressed and display a loss of H3K9me3 enrichment in *setdb1 GLKD* ovaries. (B) The genomic locations of the 20 genes which are both ectopically expressed and display a loss of H3K9me3 enrichment in *setdb1 GLKD* ovaries.

Figure S3

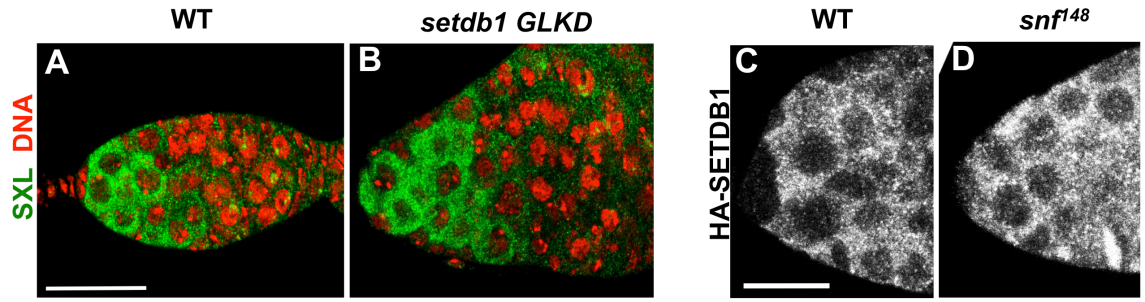

Figure S3. (Related to Figure 4) SETDB1 does not regulate SXL protein expression and SXL does not regulate SETDB1 protein expression.
(A, B) Representative confocal images of a wild-type (WT) and *setdb1 GLKD* germarium stained for DNA (red) and SXL (green). Scale bar, 25 μm. (C, D) Representative confocal images of a germaria from wild-type and *snf*^{148} females carrying a copy an endogenously HA-tagged allele of *setdb1* stained for HA. Scale bar, 12.5 μm.